INFLUENCE OF THE HYPERVELOCITY DISK PROJECTILE ORIENTATION ON DAMAGE TO TARGET: NUMERICAL SIMULATION

Andrey G. Ioilev[(1)], Vadim V. Bashurov[(1)], Olga V. Konyaeva[(1)]

[(1)] RFNC-VNIIEF, Mir Ave. 37, 607190 Sarov, Nizhnii Novgorod Reg., Russian Federation, Email: ioilev@vniief.ru

ABSTRACT/RESUME

Influence of orientation of the plate-like projectiles on their penetrating ability was studied numerically on model problems. Numerical simulation was performed using the 3-D SPH-code ELLPH, set-up was the following: titanium disk projectile, normal impact at velocity 10 km/s, "thick" and spaced aluminium targets, inclination angle of the projectile to target varied from flat-wise impact to edge-wise impact. Impact of spherical aluminium, titanium and steel projectiles was simulated also to compare with. The final dimensions and volume of crater in the aluminium blocks were considered as indicators of the impact effectiveness. The most definite difference is obtained for the spaced target: effectiveness of the disk impact changes from nearly equal to that of aluminium spherical projectile for flat-wise impact to two fold greater than that of steel spherical projectile for edge-wise impact.

1. INTRODUCTION

Within the nearest future, the International Space Station (ISS) shall be the largest artificial object operating at Low Earth Orbit for many years, so the threat of impact of meteoroids and hypervelocity particles of space debris (debris of fractured spacecrafts and launchers, see *D.J.Kessler, S.Y.Su, eds. (1985)*) is real for it. Inhabited modules of the ISS, both under operation or under development, must be protected against meteoroids and space debris to provide safety of the ISS international crew.

In space debris environment models ORDEM2000 (*J.-C.Liou, et al. (2001)*), Master'99 (*H.Sdunnus, et al. (2001)*) and SPDA-E (*A.I.Nazarenko and I.L.Menshikov (2001)*) that are usually used in evaluation of effectiveness of the protection, the space debris particles are treated as spherical aluminium projectiles, impact velocity could be as high as 12-15 km/s. For example, ORDEM2000 predicts for the ISS mean impact velocity 10.8 km/s and 9.8 km/s for the space debris particles of size 1-10 mm and 10-100 mm respectively (*J.R.Theall, et al. (2001)*). Aluminium was chosen as a typical material of the space debris particles basing on estimates of fraction of materials (aluminium, steel, titanium, plastics and composites, etc.) in the sources of space debris. Spherical shape of the space debris particles was postulated in the models on the basis of the following considerations:

1. This is the simplest shape, it is unambiguously characterised by only one dimension (e.g., diameter).
2. Results of impact of the spherical projectile to the target do not depend on its orientation.
3. Results of hypervelocity impact to the target are considered to be governed by the impact velocity and the projectile mass with only weak dependence on the projectile shape.

The first two considerations are indisputable. The third one is based on the energy similarity (see, e.g., *J.K.Diens and J.M.Walsh (1970)*), which seems reasonable for the impact velocity typical for meteoroids (>20 km/s). However, for the impact parameters typical for the space debris, geometry and material of the projectile and the target could play significant role.

Study of influence of the projectile shape (sphere, disk and rod, prolate and oblate ellipsoid) has been performed already (see, e.g., *J.W.Gehring (1970)*, *D.L.Orphal, et al. (1993)*, *F.K.Schaefer, et al. (2001)*). However, in the reported experiments projectile was oriented mainly without inclination to provide axis-symmetrical impact conditions. Systematic study of influence of orientation of the plate-like projectiles on results of hypervelocity impact to the target has not been performed yet.

Currently, hypervelocity projectiles (velocity >9-10 km/s) are formed by shaped charges (*J.Bol and W.Fucke (1997)*, *J.Walker, et al. (1995)),* or they are accelerated using special orifice at the LGG muzzle (*M.B.Boslough, et al. (1993)*, *L.C.Chhabildas, et al. (1993)*, *L.C.Chhabildas, et al. (1995)*) or by the three-stage blast launcher (*V.A.Raevsky, et al. (1997)*, *A.Geille (1997)*). Sometimes, tumbling of a thin disk-projectile is observed at large flight distances (dozens of diameters) (see, e.g., *M.B.Boslough, et al. (1993)*, *E.L.Christiansen and J.H.Kerr (1997)*). On the other side, orientation of the plate-like space debris particles at impact is random.

So, a numerical study of influence of orientation of the plate-like projectiles on their penetrating ability was performed using the 3-D SPH-code ELLPH, a modification of code KERNEL (*A.G.Ioilev and V.V.Bashurov (2001)*). In the simulations, impact velocity of the projectile was set to 10 km/s and directed at normal to the target, titanium disk of elongation l/d=0.05 was taken as a projectile (corresponds to 1:2 scaled typical dimensions of projectile reported by

M.B.Boslough, et al. (1993), *E.L.Christiansen and J.H.Kerr (1997)*), inclination angle was varied from 0 degrees (flat-wise impact) to 90 degrees (edge-wise impact). Impact to the "thick" and spaced aluminium target was considered. Impact of spherical aluminium, titanium and steel projectiles of the same mass was simulated to provide data for comparison. The final dimensions and volume of crater in the aluminium blocks were considered as indicators of the impact effectiveness.

2. SET-UP OF NUMERICAL SIMULATION

The first set of simulations (normal impact to "thick" target by a spherical projectile of the same mass as of titanium disk in the second set: m=0.1775 g) was performed to provide data for comparison. Parameters of the simulations:

Projectile (mass m=0.1775 g):

- Spherical, titanium alloy, diameter d=4.22 mm;
- Spherical, aluminium alloy, diameter d=4.96 mm;
- Spherical, hard steel, diameter d=3.53 mm.

Impact: normal, velocity 10 km/s.

Target: aluminium block 100 mm thick, square 20×20 cm^2 in transverse plane; fixed sides.

The second set of simulations (normal impact to "thick" target by a titanium disk projectile of mass m=0.1775 g) was performed to study influence of its orientation on the penetrating ability. Parameters of the simulations:

Projectile (mass m=0.1775 g): titanium alloy, disk, diameter d=10 mm, thickness h=0.5 mm, elongation h/d=0.05.

Impact: normal, velocity 10 km/s.

Inclination of the projectile (angle between its axis and a normal to the target) was varied: α=0°; 15°; 30°; 45°; 60°; 75° and 90°.

Target: aluminium block 100 mm thick, square 20×20 cm^2 in transverse plane; fixed sides.

Simulations were performed up to time 18 μs. Material of projectiles and target was modelled using the Mie-Gruneisen equation of state (EOS) with the Murnaghan approximation of "cold" pressure (*Ya.B.Zel'dovich and Yu.P.Raizer (1966)*, *F.D.Murnaghan (1951)*). A simple von Mises model with constant Poisson ratio ν and yield strength Y was used to model elastic-plastic properties, the local criterion of splitting at negative pressure p_{crit} was used to model fracture. Parameters are presented in Table, reference static data (*I.S.Grigoriev, Ye.Z.Meylikhov, eds. (1991)*) were used, EOS approximation parameters n and Γ were chosen to match Hugoniots (*L.P.Orlenko, ed. (2002)*, *R.F.Trunin, ed. (2001)*).

The third and the forth sets of simulations were repetitions of the first and the second sets respectively, but with the other target (simulations performed up to time 20 μs):

- aluminium alloy sheet 3.77 mm thick, square 20×20 cm^2 in transverse plane; fixed sides;
- standoff 13 mm;
- aluminium block 100 mm thick, square 20×20 cm^2 in transverse plane; fixed sides.

Table – Parameters of the material models

Parameter	Titanium	Aluminium	Steel
ρ_0, g/cm^3	4.52	2.78	7.7
c_0, km/s	4.99	5.61	4.76
n	2.068	3.54	4
Γ	1.03	1.176	1.38
ν	0.33	0.36	0.3
Y, GPa	1.087	0.383	1.55
p_{crit}, GPa	-1.13	-0.59	-2.66

3. RESULTS OF NUMERICAL SIMULATION AND DISCUSSION

Results of the first and the second sets of simulations (impact to the "thick" target) are presented in Figs.1-3. Typical fields of materials illustrating the crater shape are presented in Figs.1 and 2. Dependence of the crater dimensions (H is the maximal depth from the front side of block x=0; A and B are the crater diameters along axes y and z respectively in plane of the front side of block x=0) and volume V on the disk inclination angle is presented in Fig.3. Data from simulations of impact of spherical aluminium, titanium and steel projectiles are also presented in Fig.3 for comparison. These simulations showed the following:

1. For impact of spherical aluminium, titanium and steel projectiles:
   - the crater diameter is practically the same in all three simulations;
   - in simulations with aluminium and titanium projectiles the crater depth is respectively 20% and 9% less than in simulations with steel projectile.
2. For impact of disk projectiles:
   - in simulation with flat-wise impact (inclination angle α=0°) the crater depth nearly equals to the crater depth in simulation with aluminium projectile of the same mass;
   - in simulation with α=45° the crater depth is minimal: ~58% of the crater depth in simulation with flat-wise impact;
   - in simulation with edge-wise impact (inclination angle α=90°) the crater depth is maximal: ~140% of the crater depth in simulation with flat-wise impact and even more than in simulation with steel projectile of the same mass;
   - in simulations with flat-wise and edge-wise impact (inclination angle α=0° and 90° respectively) y-axis diameter A nearly equals to the crater diameter in simulations with aluminium, titanium and steel projectiles of the same mass;

- in simulation with inclination angle α=45° y-axis diameter A is maximal: ~145% of the y-axis diameter A in simulations with flat-wise and edge-wise impact;
- the crater z-diameter B is practically the same for all values of inclination angle and nearly equals to the crater diameter in simulations with aluminium, titanium and steel projectiles of the same mass;
- in simulation with inclination angle α=45° displacement b of z-diameter from x-axis along y-axis is maximal and equals to ~12% of the y-axis diameter A;
- in simulations with large inclination angles (the most evident in simulation with edge-wise impact, α=90°) the crater has a typical shape: its main part is an ellipsoid with a narrow belt in z-plane (plane of orientation of the disk before impact) and a narrow belt in y-plane formed by massive slopping of the projectile material from the crater.

Results of the second and the third sets of simulations (impact to the spaced target) are presented in Figs.4-7. Typical fields of materials illustrating the secondary debris cloud at impact to the block and shape of crater in it are presented in Figs.4 and 5. Dependence of the crater dimensions (H is the maximal depth from the front side of block x=1.667 cm; A_2 and B_2 are the crater diameters along axes y and z respectively in plane of the front side of block x=1.667 cm) and the crater volume V on the disk inclination angle is presented in Fig.6. Data from simulations of impact of spherical aluminium, titanium and steel projectiles are also presented in Fig.6 for comparison. These simulations showed the following:

1. For impact of spherical aluminium, titanium and steel projectiles:
   - the maximal damage to the target is provided by the steel projectile;
   - in simulations with titanium and steel projectiles diameter of the hole in thin sheet are nearly the same, and ~12% more than in simulation with aluminium projectile;
   - in simulation with steel projectile diameter of crater in the target block is ~5% and ~25% more than in simulations with aluminium and titanium projectiles respectively;
   - in simulation with steel projectile depth of crater in the target block is ~27% and ~60% more than in simulations with aluminium and titanium projectiles respectively.
2. For impact of disk projectiles:
   - in simulations with all the inclination angles dimensions of the hole in thin sheet are 2-2.5 fold greater than the disk diameter;
   - in simulations with all the inclination angles dimensions of the hole in thin sheet are no less than diameter of the hole in simulation with spherical aluminium projectile (excluding simulation with α=90°: ~2% less), and in simulations with α=45° and 60° even more than that in simulation with spherical titanium projectile (~22% and ~20% in y-axis and ~13% and ~8% in z-axis respectively);
   - in simulations with all the inclination angles (excluding simulation with α=90°), dimensions of the crater in the target block (depth and both diameters) are no more than that in simulation with spherical titanium projectile;
   - only in edge-wise impact simulation (α=90°) the disk projectile produces greater crater in the target block than in simulation with spherical steel projectile: 2-fold greater crater depth and z-axis diameter (disk plane), and 2-fold less y-axis crater diameter.

Obtained in simulations peculiarities of the hole and the crater shapes provide ground for judging on the disk-projectile orientation before impact to target in experiments in the case of tumbling of the projectile.

The crater volume characterizes effectiveness of the projectile kinetic energy transfer to the energy of plastic flow in the block target material. From this side, impact of disk to the "thick" target at inclination angles $0 \le \alpha \le 60°$ is no more effective than impact of spherical aluminium projectile, and at all the inclination angles is less effective than impact of spherical steel projectile. Effectiveness of impact of disk to the spaced target at inclination angles $0 \le \alpha \le 60°$ is nearly the same as for impact of spherical aluminium projectile, but at edge-wise impact (α=90°) it becomes 2-fold more effective than impact of spherical steel projectile of the same mass.

4. CONCLUSIONS

Numerical study of influence of orientation of the plate-like projectiles on their penetrating ability was performed using the 3-D SPH-code ELLPH. In the simulations, 0.5 mm thick 10 mm diameter titanium disk was taken as a projectile, impact velocity of the projectile was set to 10 km/s. Impact to "thick" and spaced target was simulated, the final dimensions and volume of crater in the aluminium blocks of targets were considered as indicators of the impact effectiveness. Performed simulations showed that impact of the disk-projectile produces damage to the blocks of targets vastly depending on the projectile orientation. The damage is significantly different from damage produced by spherical projectiles of the same mass. Obtained in simulations peculiarities of the hole and the crater shapes provide ground for judging on the disk-projectile orientation before impact to target in experiments in the case of tumbling of the projectile. Impact of disk to the "thick" target at inclination angles $0 \le \alpha \le 60°$ is no more effective than impact of spherical aluminium projectile, and at all the inclination angles is

less effective than impact of spherical steel projectile. Effectiveness of impact of disk to the spaced target at inclination angles $0 \le \alpha \le 60°$ is nearly the same as for impact of spherical aluminium projectile, but at edge-wise impact ($\alpha = 90°$) it becomes 2-fold more effective than impact of spherical steel projectile.

5. REFERENCES

Bol J., Fucke W. Shaped charge technique for Hypervelocity Impact tests at 11 km/s on Space Debris Protection Shield. *II European Conf. Space Debris*, ESOC, Darmstadt, March 17-19, 1997. Proc.: ESA SP-393, P.405-411.

Boslough M.B., Ang J.A., Chhabildas L.C., Reinhart W.D., Hall C.A., Cour-Palais B.G., Christiansen E.L., Crews J.L. Hypervelocity testing of advanced shielding concepts for spacecraft against impacts to 10 km/s. *Int. J. Impact Engng.*, 1993. Vol.14. P.95-106.

Chhabildas L.C., Dunn J.E., Reinhart W.D., Miller J.M. An impact technique to accelerate flier plates to velocities over 12 km/s. *Int. J. Impact Engng.*, 1993. Vol.14. P.121-132.

Chhabildas L.C., Kmetyk L.N., Reinhart W.D., Hall C.A. Launch capabilities to 16 km/s. In: *Shock Waves in Condensed Matter*, pt.2. 1995. P.1197-1200.

Christiansen E.L., Kerr J.H. Projectile shape effects on shielding performance at 7 km/s and 11 km/s. *Int. J. Impact Engng.*, 1997. Vol.20. P.165-175.

Diens J.K., Walsh J.M. Theory of impact: some general principles and the method of Eulerian codes. In: *High Velocity Impact Phenomena.* Ed. R.Kinslow. Academic Press, NY, 1970: P.46-104.

Experimental Data on Shock-Wave Compression and Adiabatic Unloading of Condensed Matter. Ed. R.F.Trunin. Sarov, RFNC-VNIIEF, 2001.

Gehring J.W. Engineering considerations in hypervelocity impact. In: *High Velocity Impact Phenomena.* Ed. R.Kinslow. Academic Press, NY, 1970: P.463-514.

Geille A. Status of development of space debris hypervelocity explosive multi-stage launcher. *Int. J. Impact Engng.*, 1997. Vol.20. P.271-280.

Ioilev A.G., Bashurov V.V. SPH-code KERNEL: Three-dimensional numerical simulation of hypervelocity perforation. *III European Conf. Space Debris.* ESOC, Darmstadt, Germany, March 19-21, 2001. Proc.: ESA SP-473, P.629-637.

Liou J.-C., Matney M., Anz-Meador P., Kessler D.J., Jansen M., Theall J.R. The new NASA orbital debris engineering model ORDEM2000. *III European Conf. Space Debris.* ESOC, Darmstadt, Germany, March 19-21, 2001. Proc.: ESA SP-473, P.309-313.

Murnaghan F.D. *Finite Deformation of Elastic Solid*. NY, 1951.

Nazarenko A.I., Menshikov I.L. Engineering model of space debris environment. *III European Conf. Space Debris.* ESOC, Darmstadt, Germany, March 19-21, 2001. Proc.: ESA SP-473, P.293-298.

Orbital debris. Ed. D.J.Kessler, S.Y.Su, *NASA CP 2360*, Washington, D.C., 1985.

Orphal D.L., Anderson C.E., Jr, Franzen R.R., Walker J.D., Schneiderwind P.N., Majerus M.E. Impact and penetration by L/D≤1 projectiles. *Int. J. Impact Engng.*, 1993, vol.14, pp.551-560.

Physical values. Handbook. Eds. I.S.Grigoriev, Ye.Z.Meylikhov. Moscow, Energoatomizdat Publ., 1991.

Physics of Explosion. Vol.2. Ed. L.P.Orlenko. Moscow, Fizmatlit Publ., 2002.

Raevsky V.A., Bat'kov Yu.V., Kovalev N.P., et al. Explosive three-stage launcher to accelerate metal plates to velocities more than 10 km/s. *Int. J. Impact Engng.*, 1997. Vol.20. No.1-5. P.89-93.

Schaefer F.K., Herrwerth M., Hiermaier S.J., Schneider E.E. Shape effects in hypervelocity impact on semi-infinite metallic targets. *Int. J. Impact Engng.*, 2001. Vol.26. P.699-711.

Sdunnus H., Bendish J., Klinkrad H. The ESA MASTER'99 space debris and meteoroid reference model. *III European Conf. Space Debris.* ESOC, Darmstadt, Germany, March 19-21, 2001. Proc.: ESA SP-473, P.299-307.

Theall J.R., Liou J.-C., Matney M., Kessler D.J. The space debris environment for the ISS orbit. *III European Conf. Space Debris.* ESOC, Darmstadt, Germany, March 19-21, 2001. Proc.: ESA SP-473, P.429-432.

Walker J., Grosch D.G., Mullin S.A. Experimental impacts above 10 km/s. *Int. J. Impact Engng.*, 1995. Vol.17. P.903-914.

Zel'dovich Ya.B., Raizer Yu.P. *Physics of Shock Waves and High Temperature Hydrodynamic Phenomena.* Moscow, Science Publ., 1966.

6. FIGURES (click to magnify)

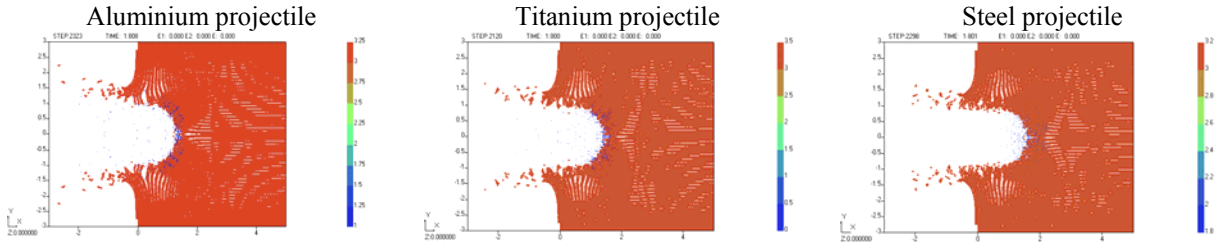

Figure 1. Field of materials in simulations of impact of spherical projectiles at the end of calculation (t=18 μs): axial cross-section (0<z<0.2 cm).

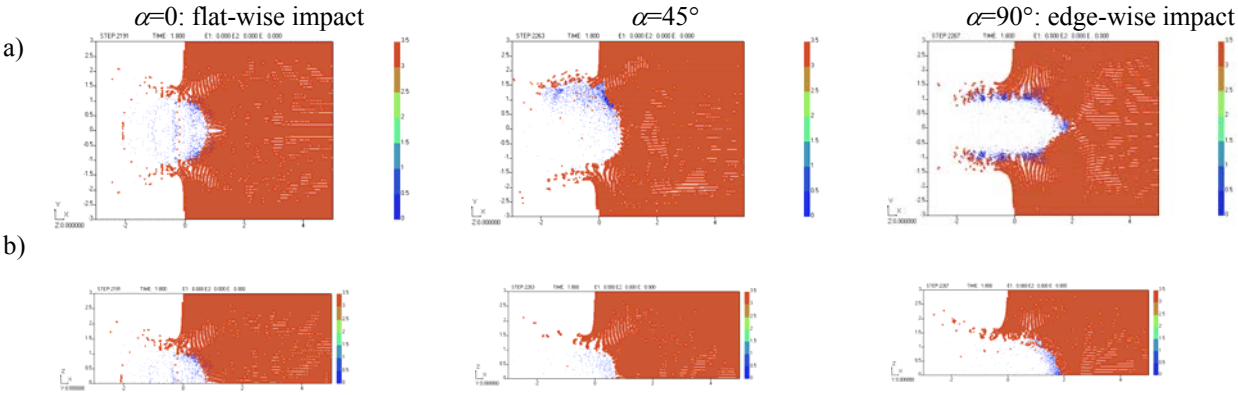

Figure 2. Field of materials in simulations of impact of titanium disk projectile at the end of calculation (t=18 μs): a) axial cross-section (0<z<0.2 cm); b) axial cross-section (0<y<0.2 cm).

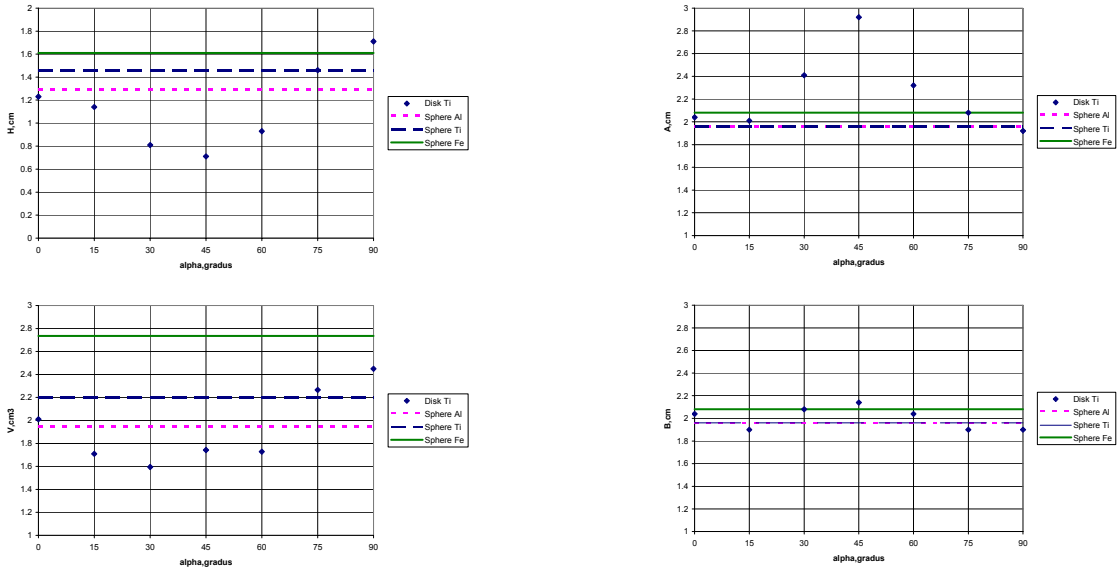

Figure 3. Dependence of the crater dimensions and volume on the disk inclination angle.

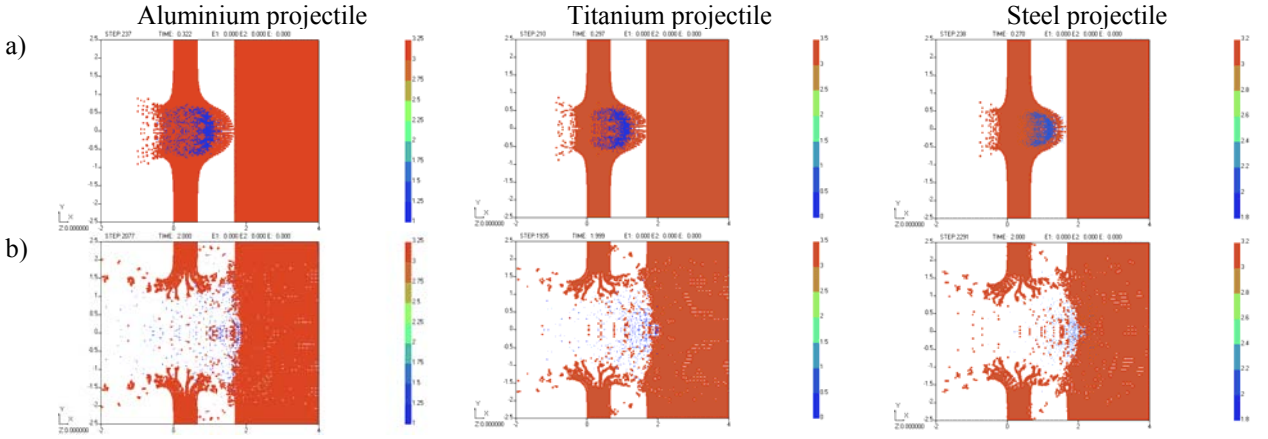

Figure 4. Field of materials in simulations of impact of spherical projectiles, axial cross-section (0<z<0.2 cm): a) at the secondary debris arrival to the target block (t≈3 μs); b) at the end of calculation (t=20 μs).

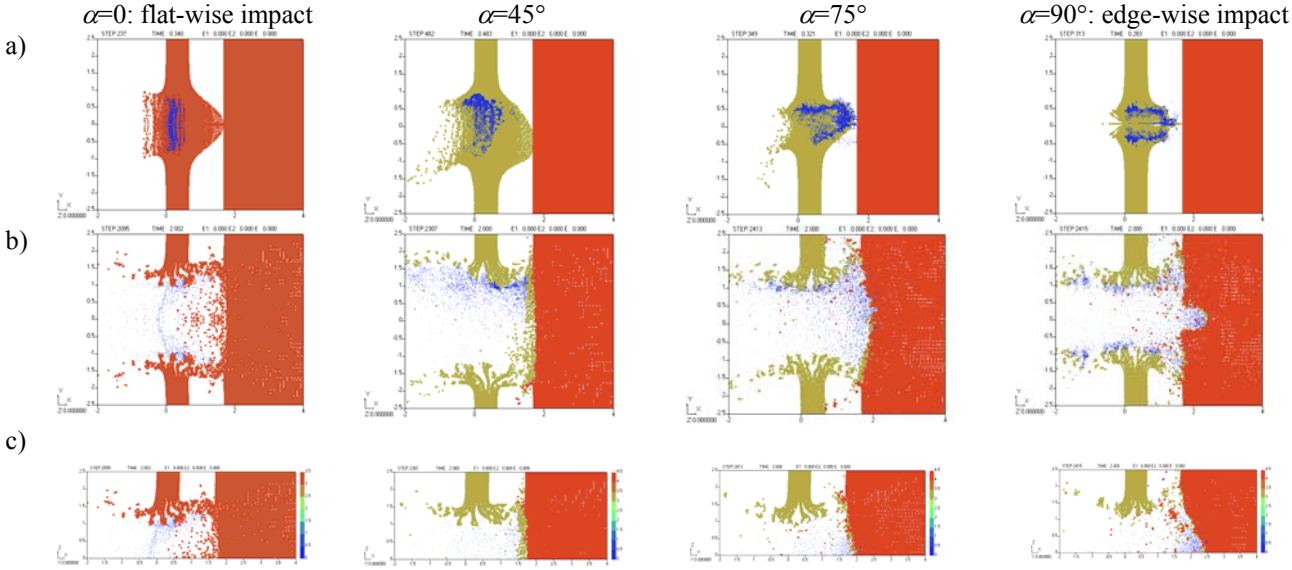

Figure 5. Field of materials in simulations of impact of titanium disk projectile (a - at the secondary debris arrival to the target block; b,c - at the end of calculation t=20 μs): a) cross-section in xy-plane (z>0); b) cross-section in xy-plane (0<z<0.2 cm); c) cross-section in xz-plane (0<y<0.2 cm).

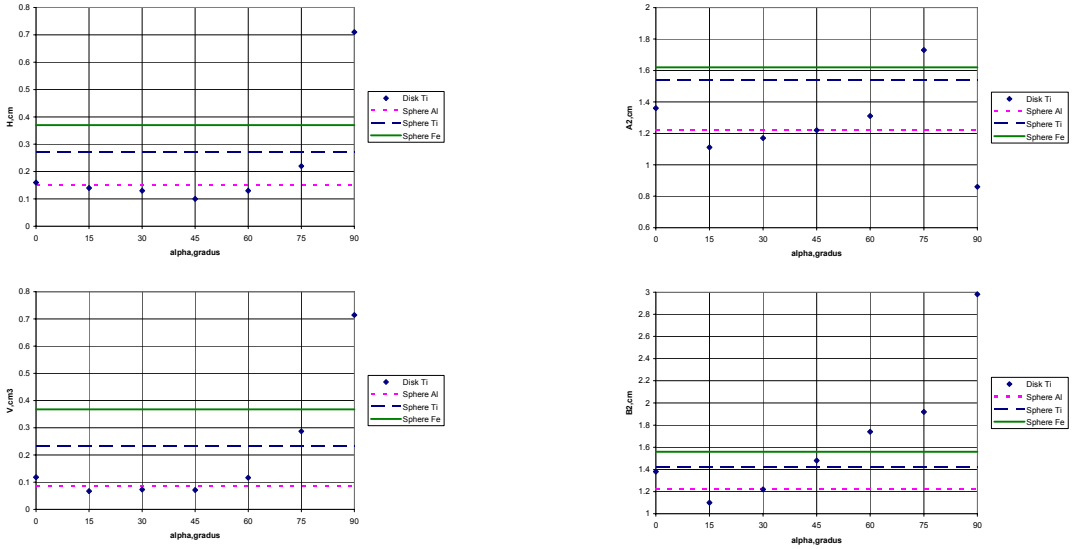

Figure 6. Dependence of the crater dimensions and volume on the disk inclination angle.